J|A|C|S
ARTICLES
Published on Web 01/28/2003

Kemp Elimination in Membrane Mimetic Reaction Media: Probing Catalytic Properties of Catanionic Vesicles Formed from Double-Tailed Amphiphiles

Jaap E. Klijn and Jan B. F. N. Engberts*

Contribution from the Physical Organic Chemistry Unit, Stratingh Institute, University of Groningen, Nijenborgh 4, 9747 AG Groningen, The Netherlands

Received July 19, 2002; E-mail: J.B.F.N.Engberts@chem.rug.nl

Abstract: The rate-determining deprotonation of 5-nitrobenzisoxazole (Kemp elimination) by hydroxide is efficiently catalyzed by vesicles formed from dimethyldioctadecylammonium chloride ($C_{18}C_{18}^+$). Gradual addition of sodium didecyl phosphate ($C_{10}C_{10}^-$) leads to the formation of catanionic vesicles, which were characterized by cryo-electron microscopy, and their main phase transition temperatures (DSC) and ζ-potentials. Increasing percentages of $C_{10}C_{10}^-$ in the vesicular bilayers decrease the catalysis of the Kemp elimination. A detailed kinetic analysis, supported by consideration of substrate binding site polarities and counterion binding percentages, suggest that the catalytic effects of $C_{18}C_{18}^+/C_{10}C_{10}^-$ catanionic vesicles are primarily determined by the binding of catalytically active hydroxide ions to the vesicular surface area. The formation of neutral microdomains between 10 and 30 mol % of $C_{10}C_{10}^-$ in the bilayer, as revealed by DSC, is not apparent from the catalytic effects found for these vesicles. Interestingly, the catalytic effects observed for 50 mol % $C_{10}C_{10}^-$ in the catanionic vesicles indicate an asymmetric distribution of $C_{18}C_{18}^+$ and $C_{10}C_{10}^-$ over the bilayer leaflets. The overall kinetic results illustrate the highly complex mix of factors which determines catalytic effects on reactions occurring in biological cell membranes.

Introduction

Micelles have been extensively studied with respect to their catalytic properties toward a variety of organic reactions.[1−9] Some reactions (for example, hydrolysis reactions of (activated) esters) are inhibited by the presence of micellar aggregates.[10] Studies on vesicular catalysis[11,12] are generally more complex because, contrary to micelles, vesicles are usually not thermodynamically stable and experiments yield more scattering in the data.

In general, two effects lead to the catalysis of bimolecular reactions in micellar and vesicular aggregates.[2] The first effect comes from substrate−aggregate binding. Charged micelles and vesicles provide a good environment for hydrophobic and oppositely charged molecules to bind, thereby increasing the chances of two substrates to meet and react because the effective reaction volume is reduced. Particularly when one of the two reactants can bind as a counterion to the aggregate, efficient catalysis is found, because the concentration of headgroups in the Stern layer of micelles is in the order of 3 to 5 M.[10] By contrast, when only one of the two reactants binds to the aggregate, inhibition is observed.

The second effect results from the decreased local polarity at the micellar and vesicular binding sites compared to water. Of course, the latter effect is only beneficial when the organic reaction is accelerated in less polar environments.

Vesicles can be used as mimics for aspects of the chemistry of the much more complicated biological membranes. Biological membranes are extremely complex mixtures of mainly lipids, steroids, and proteins.[13−15] In addition to this complexity, both leaflets of the membrane have different compositions. But also within the leaflets the distribution of the different lipids over the membrane is believed to be nonrandom.[16−22]

(1) Grieco, P. A. *Organic Synthesis in Water*; Thomson Science: London, 1998.
(2) Bunton, C. A.; Nome, F.; Quina, F. H.; Romsted, L. S. *Acc. Chem. Res.* **1991**, *24*, 357−364.
(3) Berezin, I. V.; Martinek, K.; Yatsimirskii, A. K. *Russ. Chem. Rev. (Engl. Transl.)* **1973**, *42*, 787.
(4) Engberts, J. B. F. N.; Blandamer, M. J. *Chem. Commun.* **2001**, 1701−1708.
(5) Otto, S.; Engberts, J. B. F. N. *Pure Appl. Chem.* **2000**, *72*, 1365−1372.
(6) Bunton, C. A.; Wright, S.; Holland, P. M.; Nome, F. *Langmuir* **1993**, *9*, 117−120.
(7) Mashraqui, S. H.; Kumar, S.; Mudaliar, C. D. *Bull. Chem. Soc. Jpn.* **2001**, *74*, 2133−2138.
(8) Iglesias, E. *J. Phys. Chem. B* **2001**, *105*, 10 295−10 302.
(9) Bravo, C.; Leis, J. R.; Peña, M. E. *J. Phys. Chem.* **1992**, *96*, 1957−1961.
(10) Buurma, N. J.; Herranz, A. M.; Engberts, J. B. F. N. *J. Chem. Soc., Perkin Trans. 2* **1999**, 113−119.
(11) Perez-Juste, J.; Hollfelder, F.; Kirby, A. J.; Engberts, J. B. F. N. *Org. Lett.* **2000**, *2*, 127−130.
(12) Rispens, T.; Engberts, J. B. F. N. *Org. Lett.* **2001**, *3*, 941−943.
(13) Gennis, R. B. In *Biomembranes: Molecular Structure and Function*; Springer-Verlag: New York, 1989; pp 20−35.
(14) Darnell, J.; Lodish, H.; Baltimore, D. In *Molecular Cell Biology*; Scientific American Books: New York, 1990; pp 491−499.
(15) Alberts, B.; Bray, D.; Lewis, J.; Raff, M.; Roberts, K.; Watson, J. D. In *Molecular Biology of the Cell*; Garland Publishing: New York, 1994; pp 477−485.
(16) London, E.; Brown, D. A. *Biochim. Biophys. Acta* **2000**, *1508*, 182−195.
(17) Pralle, A.; Keller, P.; Florin, E. L.; Simons, K.; Horber, J. K. H. *J. Cell Biol.* **2000**, *148*, 997−1007.
(18) Simons, K.; Ikonen, E. *Nature* **1997**, *387*, 569−572.
(19) Simons, K.; Ikonen, E. *Science* **2000**, *290*, 1721−1726.
(20) Rietveld, A.; Simons, K. *Biochim. Biophys. Acta* **1998**, *1376*, 467−479.
(21) Schroeder, R. J.; Ahmed, S. N.; Zhu, Y. Z.; London, E.; Brown, D. A. *J. Biol. Chem.* **1998**, *273*, 1150−1157.
(22) Ahmed, S. N.; Brown, D. A.; London, E. *Biochemistry* **1997**, *36*, 10 944−10 953.

Scheme 1. Kemp Elimination Reaction

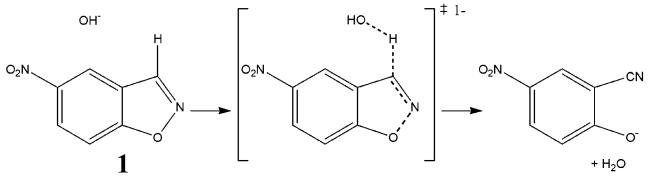

On the basis of these considerations, we decided to examine the catalytic properties of catanionic vesicles prepared from structurally simple amphiphiles. The kinetic probe that we employed is the bimolecular, base-catalyzed, rate determining deprotonation of 5-nitrobenzisoxazole (**1**; Kemp elimination;[23] Scheme1). The potential of this reaction for probing biochemically relevant reaction conditions has already been demonstrated, particularly by Kirby et al.[24] The reaction can also act as model reaction for deprotonation reactions in biological membranes. The rate of deprotonation is much faster in an apolar environment than in a polar environment.

Cationic vesicles in basic aqueous solutions catalyze the deprotonation because not only the local polarity is decreased, but also the local concentration of base is increased.[11] In the present study, particular focus was placed on the question how the catalysis is affected by gradually mixing cationic vesicles with anionic bilayer forming amphiphiles and which factors determine the changes in catalytic efficiency. Our results may have relevance for a better understanding of the chemistry occurring in the living cell, for example in the membrane of the mitochondrion.[25]

Experimental Section

Materials. Dimethyldioctadecylammonium chloride (>97%), sodium chloride (p.A.), sodium hydroxide (titrisol) and pyrene (>99%) were purchased from Fluka, Merck (2x) and Aldrich, respectively. The E_T(30)-probe (2,6-diphenyl-4-(2,4,6-triphenyl-1-pyridino) phenoxide) was kindly provided by Prof. Ch. Reichardt (University of Marburg). 5-Nitrobenzisoxazole (**1**) was a generous gift from Dr. F. Hollfelder and Prof. A. J. Kirby[26] of the University Chemical Laboratory (Cambridge, UK).

All chemicals were used as received. Sodium didecyl phosphate was synthesized according to a literature procedure.[27] Doubly distilled water was used for all solutions.

Kinetic Experiments. Kinetic experiments were performed using an Applied Photophysics SX-18MV Stopped-Flow Reaction Analyzer (Leatherhead, UK) thermostated with a Neslab RTE−111 water bath. The deprotonation reaction was followed at 380 nm. The temperature was 15.0 ± 0.1 °C unless stated otherwise. Stock solutions of approximately 30 mM total amphiphile concentration were prepared by weighing the needed amounts of amphiphile. Water was added to the appropriate volume and the solution was kept in a water bath at 50 °C for at least 45 min. Then the solution was sonicated using a tip sonicator (Branson Sonifier B15−P) at 50 °C for 6 min (or longer if not all solid material was solubilized). Subsequently, the stock solution was extruded 11 times through a 400 nm filter using a mini-extruder (Avanti Polar Lipids, Alabaster, AL) at 50 °C. Finally, the stock solution was diluted to the desired concentrations and sodium hydroxide from a 1 M stock solution was added so that the total concentration of sodium hydroxide was 4.5 mM. Control experiments were performed to see whether "aging" of the solution was a factor of importance, but no effect was found over a period of 15 h. Stock solutions of **1** were prepared by dissolving 0.00033 g **1** in 100 mL of water (2×10^{-5} M). For each stock solution the UV−vis spectra before and after reaction were recorded to check the concentration and purity.

In all the kinetic runs the concentration of hydroxide was 2.25 mM and the concentration of **1** was 1×10^{-5} M (please note that in the stopped-flow apparatus one volume unit with **1** is mixed with one volume unit of the alkaline vesicular solution).

Differential Scanning Microcalorimetry. DSC scans were taken on a VP-DSC apparatus (Microcal, Northhampton, MA) with a scan rate of 1 °C min^{-1}. Solutions were prepared similarly as described for the kinetic experiments. The total amphiphile concentration was 2 mM and the total concentration of sodium hydroxide was 4.5 mM. Five scans were performed between 5 °C and 100 °C. The reference cell was filled with water. The solutions were allowed to equilibrate at 1 °C for 2 h between successive scans. A water scan was subtracted using Microcal Origin software. The first scan was neglected due to the thermal history of the machine, but the other scans were all identical.

ζ-Potentials. Mobilities were measured using a Malvern Zetasizer 5000 (Malvern, UK). ζ-potentials were then calculated using the Smoluchowsky limits. All solutions used contained 5 mM total amphiphile concentration and 2.25 mM NaOH and were prepared as described for the kinetic experiments, except that they were prepared at 5 mM and the solutions were not extruded. All experiments were performed around 15 °C.

Cryo-Electron Microscopy. A small drop of the 20 mM amphiphile solution was deposited on a glow discharged holey carbon-coated grid. After blotting away the excess of amphiphile, the grids were plunged in liquid ethane. Frozen hydrated specimen were mounted in a GatAn (model 626) CRYO−STAGE and examined in a Philips CM 120 cryo electron microscope operating at 120 kV.

E_T(30)-Probe. All vesicular solutions were prepared as described for the kinetic experiments. The concentration of sodium hydroxide was 2.25 mM. 4 μL of a saturated solution of the E_T(30)-probe in acetonitrile was added to a vesicular solution and the wavelength of maximum absorption was measured on a Perkin-Elmer λ5 spectrophotometer at least five minutes after mixing the solutions. The E_T(30) value was then calculated as described[28] using eq 1

$$E_T(30) = hc\tilde{\nu}_{max}N_A = \frac{28591}{\lambda_{max}} \quad (1)$$

In this equation h, c, and N_A are Planck's constant, the speed of light and Avogadro's number, respectively. λ_{max} and ν_{max} are the wavelength (in nm) and frequency of the maximum absorption of the E_T(30) probe, respectively.

Vesicle concentrations were chosen such that λ_{max} did not change with concentration indicating that the probe was fully bound.

Steady-State Fluorescence. Pyrene was dissolved in water and filtered at least 1 day after dissolution. This solution was then diluted once. No excimers were present since steady-state fluorescence showed no peak near 450 nm, characteristic of pyrene excimers.[29] Pyrene was present at concentrations lower than 10^{-6} M. Steady-state fluorescence spectroscopic measurements were performed using a SLM SPF-500C spectrofluorometer equipped with a thermostated cell holder and a magnetic stirring device. Measurements were initiated at least 15 min after mixing the vesicular and pyrene solution. The instrument settings were as follows: excitation wavelength, 335 nm; slid width 5 nm. The emission spectrum was recorded from 371 to 386 nm (slit width, 1 nm; step size 0.20 nm; filter 2). The intensities of the first (around 372 nm) and third peak (around 385 nm) were determined.

(23) Kemp, D. S.; Casey, M. L. *J. Am. Chem. Soc.* **1973**, *95*, 6670−6680.
(24) Hollfelder, F.; Kirby, A. J.; Tawfik, D. S. *Nature* **1996**, *383*, 60−63.
(25) Demirel, Y.; Sandler, S. I. *Biophys. Chem.* **2002**, *97*, 87−111.
(26) Hollfelder, F.; Kirby, A. J.; Tawfik, D. S.; Kikuchi, K.; Hilvert, D. *J. Am. Chem. Soc.* **2000**, *122*, 1022−1029.
(27) Wagenaar, A.; Rupert, L. A. M.; Engberts, J. B. F. N.; Hoekstra, D. *J. Org. Chem.* **1989**, *54*, 2638−2642.
(28) Reichardt, C. *Chem. Rev.* **1994**, *94*, 2319−2358.
(29) Berlman, I. B. *Handbook of Fluorescence Spectra of Aromatic Molecules*; Academic Press: New York, 1965.

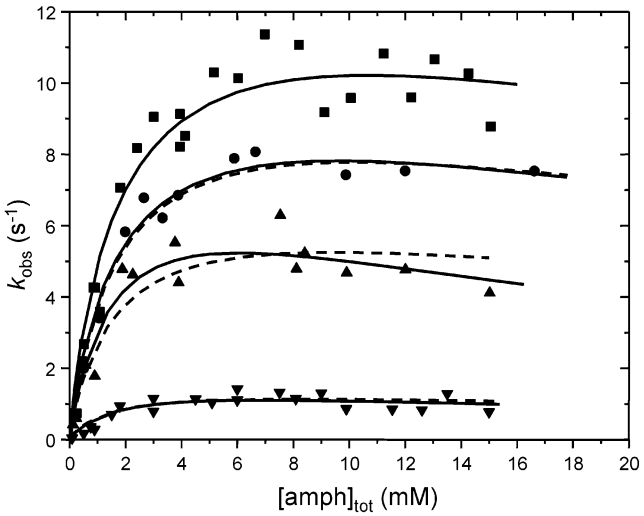

Figure 1. Experimental values for k_{obs} as a function of the total amphiphile concentration. The solid lines are least-squares fits of eqs 6 and 8 to the data using $K_{OH}^{Cl} = 2.4$ and $\beta_{excess} = 0.8$. The dashed lines are least-squares fits of eqs 6 and 8 to the data using $K_S = 23.4\ M^{-1}$ and $k_{ves} = 495\ s^{-1}$.The following percentages denote the percentage of $\mathbf{C_{10}C_{10}}^-$ as a function of the total amphiphile concentration. (■) 0 mol %; (●) 10 mol %; (▲) 20 mol %; (▼) 35 mol %.

Results and Discussion

Vesicular Catalysis. The Kemp elimination is efficiently catalyzed by vesicles formed from dimethyldioctadecylammonium chloride ($\mathbf{C_{18}C_{18}}^+$). At 15 °C and in the presence of 2.25 mM of sodium hydroxide, the observed rate increase amounts to a factor of ca. 100, consistent with our previous studies.[11] A more detailed kinetic analysis (vide infra) taking into account the binding efficiency of **1** to the vesicles and the vesicular reaction volume, reveals that the vesicular rate constant is 65 times higher than the rate constant in water.

We have examined how the observed pseudo-first-order rate constant (k_{obs}, s^{-1}) for deprotonation of **1** in vesicles formed from $\mathbf{C_{18}C_{18}}^+$ responds to a gradual addition of anionic bilayer-forming sodium didecyl phosphate ($\mathbf{C_{10}C_{10}}^-$). The combination of a cationic amphiphile with long tails and an anionic amphiphile with short tails was chosen to avoid precipitation of the catanionic mixture.[30] Figure 1 shows plots of k_{obs} versus the total amphiphile concentration ([amph]$_{tot}$) up to ca. 16 mM. As anticipated on the basis of the decreasing positive surface charge potential of the vesicles, k_{obs} decreases with increasing concentration of $\mathbf{C_{10}C_{10}}^-$. However, the observed rate profiles are similar for all amphiphile mixtures. Upon increasing [amph]$_{tot}$ there is initially a sharp increase of k_{obs} to a maximum value depending on the percentage of $\mathbf{C_{10}C_{10}}^-$ in the bilayer, whereas k_{obs} then slowly decreases. This type of behavior is characteristic for micellar and vesicular catalysis of bimolecular reactions.[31]

Cryo-Electron Microscopy. Before analyzing the kinetic data obtained for the vesicles formed by the $\mathbf{C_{18}C_{18}}^+/\mathbf{C_{10}C_{10}}^-$ mixtures, we will further characterize these bilayer vesicles. In Figure 2 cryo-EM pictures are shown for vesicles of different composition. Figure 2a clearly shows only "lens-shaped" vesicles,[32] i.e., vesicles that are round when looked from the top, but that are strongly flattened when looked from aside. At 10 mol % $\mathbf{C_{10}C_{10}}^-$ (Figure 2b) the cryo-EM picture shows more or less the same structures, except that sometimes one of the two "lenses" has extra curvature. At 40 mol % $\mathbf{C_{10}C_{10}}^-$ (Figure 2c) angular spherical vesicles are observed. This angularity has been observed before[32] and is due to the fact that the vesicles are below their T_m when they are vitrified. This angularity is also observed for 50 mol % $\mathbf{C_{10}C_{10}}^-$ (Figure 2d), but now also clustering is observed due to the absence of strong electrostatic repulsion between the vesicles since the vesicles are almost overall neutral. At 70 mol % $\mathbf{C_{10}C_{10}}^-$ (Figure 2e) only spherical vesicles are observed.

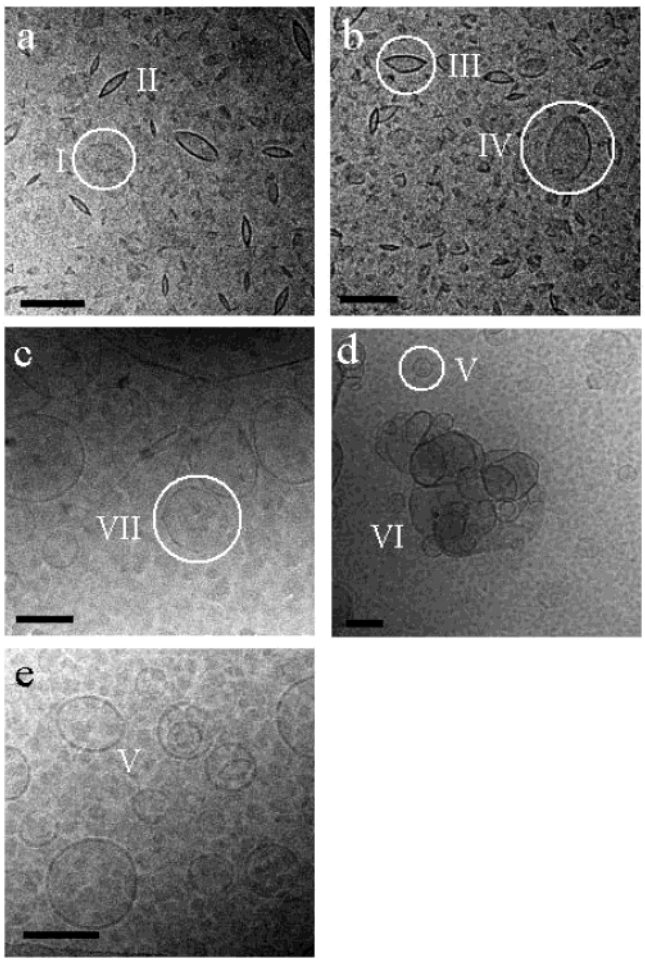

Figure 2. Cryo-EM pictures of mixtures of $\mathbf{C_{18}C_{18}}^+$ and $\mathbf{C_{10}C_{10}}^-$. The letter denotes the percentage of $\mathbf{C_{10}C_{10}}^-$ as a function of the total amphiphile concentration. (a) 0 mol %; (b) 10 mol %; (c) 40 mol %; (d) 50 mol %; (e) 70 mol %. Explanation of numbers: (I) top view; (II) side view; (III) side view where one "lens" has extra curvature; (IV) top view, but slightly tilted; (V) spherical vesicle; (VI) clustering of vesicles; (VII) angular vesicle. The bar represents 100 nm.

Differential Scanning Microcalorimetry. An important feature of vesicles is that alkyl tails of the amphiphiles can be in two states: a highly ordered, rigid (gellike) state and a more fluid (liquid-crystalline) state. The temperature for this morphological change is typical for each amphiphile and is called the main phase transition temperature (T_m). Differential scanning microcalorimetry (DSC) is a useful technique for measuring the

(30) Adding sodium dioctadecyl phosphate or sodium dioleyl phosphate to $\mathbf{C_{18}C_{18}}^+$ leads to precipitation.
(31) Romsted, L. S. In *Micellization, Solubilization and Microemulsion*; Mittal, K. L., Ed.; Plenum Press: New York, 1977; pp 509−530.
(32) Andersson, M.; Hammarstrom, L.; Edwards, K. *J. Phys. Chem.* **1995**, *99*, 14 531−14 538.

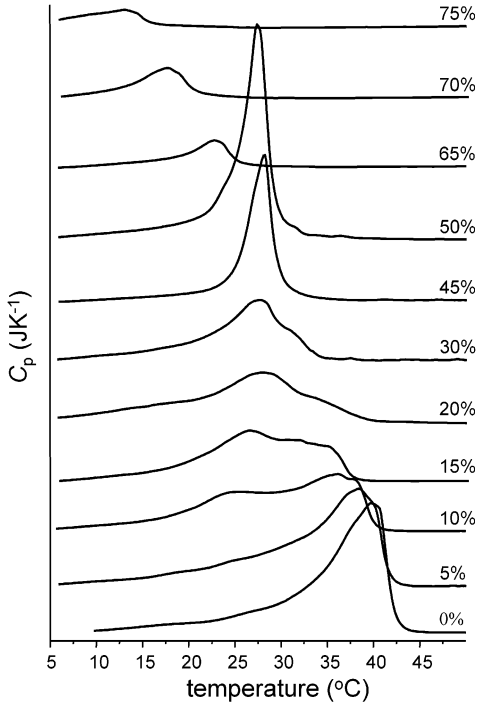

Figure 3. Heating scans for mixtures of $\mathbf{C_{18}C_{18}}^+$ and $\mathbf{C_{10}C_{10}}^-$ vesicles. The number denotes the percentage of $\mathbf{C_{10}C_{10}}^-$ as a function of the total amphiphile concentration. Lines have been elevated for clarity.

phase transition temperature. The T_m for $\mathbf{C_{18}C_{18}}^+$ vesicles is 40 °C (Figure 3) which agrees with the literature[33] and for $\mathbf{C_{10}C_{10}}^-$ vesicles 8 °C.[27] In Figure 3, the scans for pure $\mathbf{C_{18}C_{18}}^+$ and mixtures of $\mathbf{C_{18}C_{18}}^+$ with $\mathbf{C_{10}C_{10}}^-$ are shown. The decrease of T_m upon addition of $\mathbf{C_{10}C_{10}}^-$ is remarkable since the addition of anionic single-tailed, micelle-forming amphiphiles is known to increase the T_m.[34] At 10 mol % of $\mathbf{C_{10}C_{10}}^-$ a second peak arises around 27 °C and this peak becomes more prominent until it reaches a maximum at 50 mol % $\mathbf{C_{10}C_{10}}^-$. At the same time, the peak at 40 °C decreases in size and slowly moves toward 30 °C, disappearing at 30 mol % of $\mathbf{C_{10}C_{10}}^-$. Above 50 mol % $\mathbf{C_{10}C_{10}}^-$, there is only one peak and upon increasing the amount of anionic amphiphile the peak shifts toward 8 °C. Above 75 mol % $\mathbf{C_{10}C_{10}}^-$, it was impossible to perform DSC scans since precipitation took place a few minutes after preparation of the vesicles.

These results can be explained in terms of the presence of neutral microdomains between 10 mol % and 30 mol % $\mathbf{C_{10}C_{10}}^-$. The peak arising in the range 23−27 °C must have a 1:1 cationic:anionic amphiphile ratio because it is the only peak that is observed at 50 mol % $\mathbf{C_{10}C_{10}}^-$. Therefore, we contend that at 10 mol % $\mathbf{C_{10}C_{10}}^-$ neutral microdomains are formed besides a mainly cationic phase. At 30 mol % $\mathbf{C_{10}C_{10}}^-$, these microdomains resolve into one homogeneous phase again. At the same time as the microdomains are formed, the cationic domains possess an increasing amount of $\mathbf{C_{10}C_{10}}^-$ randomly mixed-in because the peak in the DSC scans progressively moves toward lower temperatures. Microdomain formation has been observed before in single-tailed catanionic surfactant mixtures.[35]

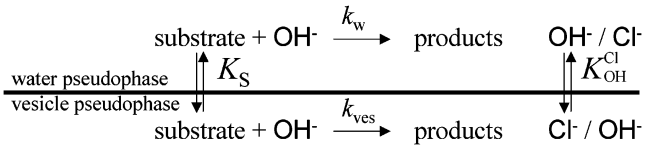

Figure 4. Schematic representation of the kinetic model used. K_S is the binding constant of the organic substrate to vesicular pseudophase, k_w is the rate constant in water, k_{ves} is the vesicular rate constant and K_{OH}^{Cl} is the binding constant of OH^- to the vesicular pseudophase.

In principle, the appearance of two peaks in the DSC scans could also be due to the presence of two types of vesicles in solution, but this option was ruled out because all cryo-EM pictures show only one type of vesicle present. If there would be two types of vesicles in solution, then one would expect to see both cationic ("lens"-type vesicles; Figure 2a) and catanionic vesicles (aggregates of spherical vesicles; Figure 2d) because only the peaks corresponding to these type of bilayers are observed in the DSC scans. Because this is not the case, the peak in the DSC scan at 27 °C should belong to neutral microdomains.

Kinetic Analysis. The rate profiles shown in Figure 1 can be analyzed in terms of the pseudophase model with ion exchange developed by Romsted et al.[31] (Figure 4). In this model there are two phases; an aqueous phase and a vesicular phase. In the apolar vesicular phase the rate constant is much higher than in the aqueous phase. Because **1** prefers to be in the vesicular phase, and the base prefers to bind to the cationic surface the two reagents are efficiently brought together.

The observed rate constant (k_{obs}) can be described by eq 2

$$k_{obs}[P]_{tot} = k_w[OH]_w[P]_w + k'_{ves}[OH]_{ves}[P]_{ves} \qquad (2)$$

In this equation $[P]_{tot}$, $[P]_w$, and $[P]_{ves}$ are the total, aqueous and vesicular probe concentrations, respectively. The total probe concentration is equal to the sum of probe concentrations in the aqueous and vesicular phase. k_w and k'_{ves} are the rate constants in the aqueous and the vesicular phase, respectively. $[OH]_w$ and $[OH]_{ves}$ are the hydroxide concentrations in the aqueous and the vesicular phase. The total hydroxide concentration is equal to the sum of hydroxide concentrations in the aqueous and vesicular phase. The binding constant K_S (eq 3) of the probe to the vesicles is expressed in terms of the total amphiphile concentration ($[amph]_{tot}$), i.e., the sum of the concentration of cationic and anionic amphiphiles

$$K_S = \frac{[P]_{ves}}{[P]_w[amph]_{tot}} \qquad (3)$$

Combining and rewriting eqs 2 and 3 with eqs 4 and 5 gives eq 6

$$k_{ves} = k'_{ves}[amph]_{tot} \qquad (4)$$

$$m_{OH} = \frac{[OH]_{ves}}{[C_{18}C_{18}^+]_{excess}} \qquad (5)$$

(33) Feitosa, E.; Barreleiro, P. C. A.; Olofsson, G. *Chem. Phys. Lipids* **2000**, *105*, 201−213.
(34) Kacperska, A. *J. Therm. Anal.* **2000**, *61*, 63−73.
(35) Dubois, M.; Deme, B.; Gulik-Krzywicki, T.; Dedieu, J. C.; Vautrin, C.; Desert, S.; Perez, E.; Zemb, T. *Nature* **2001**, *411*, 672−675.

$$k_{obs} = \frac{k_w[OH]_{tot} + (k_{ves}K_S - k_w)m_{OH}[C_{18}C_{18}^{+}]_{excess}}{1 + K_S[amph]_{tot}} \quad (6)$$

$[\mathbf{C_{18}C_{18}}^{+}]_{excess}$ is the concentration of $\mathbf{C_{18}C_{18}}^{+}$ that is present in the bilayer in excess to the amount of anionic amphiphile and can be described by eq 7

$$[C_{18}C_{18}^{+}]_{excess} = (1 - 2\alpha)[amph]_{tot} \quad (7)$$

In this eq α is the ratio of anionic amphiphile to the total amphiphile concentration.

Because one cannot measure the vesicular hydroxide concentration, it can be calculated using eq 8[36]

$$m_{OH}^{2} + m_{OH}\left[\frac{[OH]_{tot} + K_{OH}^{Cl}[Cl]_{tot}}{(K_{OH}^{Cl} - 1)[C_{18}C_{18}^{+}]_{excess}} + \beta_{excess}\right] - \left[\frac{\beta_{excess}[OH]_{tot}}{(K_{OH}^{Cl} - 1)[C_{18}C_{18}^{+}]_{excess}}\right] = 0 \quad (8)$$

In this eqation K_{OH}^{Cl} is the ratio of hydroxide and chloride ions bound to the bilayer (eq 9)

$$K_{OH}^{Cl} = \frac{[Cl]_{ves}[OH]_w}{[Cl]_w[OH]_{ves}} \quad (9)$$

β_{excess} is the ratio of counterions that are bound to the *excess* of $\mathbf{C_{18}C_{18}}^{+}$ and is given by eq 10

$$\beta_{excess} = \frac{[OH]_{ves} + [Cl]_{ves}}{[C_{18}C_{18}^{+}]_{excess}} \quad (10)$$

The *total* counterion binding (β_{tot}) includes the binding of $\mathbf{C_{10}C_{10}}^{-}$ to the total amount of cationic amphiphiles and is given by eq 11

$$\beta_{tot} = \frac{[OH]_{ves} + [Cl]_{ves} + \alpha[amph]_{tot}}{[C_{18}C_{18}^{+}]} = \frac{\alpha + \beta_{excess}(1 - 2\alpha)}{1 - \alpha} \quad (11)$$

An important assumption is that the counterion binding over the amphiphile concentration range remains constant. This has been proven for micelles,[37] and we assume this is also true for vesicular solutions.

Ruan et al.[38] calculated the binding constant K_{OH}^{Cl} by rewriting eqs 6 and 8 into a linear equation where $1/k_{obs}$ is a function of the total chloride concentration (Figure 5). Then K_{OH}^{Cl} can be calculated by taking the ratio of the slope to the intercept (eq 12)

$$K_{OH}^{Cl} = \frac{\text{slope}}{\text{intercept}} \times [OH]_{tot} \quad (12)$$

However, due to some mathematical assumptions,[38] this linear equation is only valid when $[\mathbf{C_{18}C_{18}}^{+}]_{excess}$ is smaller than 0.5 mM and the total chloride concentration is higher than 4.5 mM. As can be seen in Figure 5, the main problem with these fits is the small value of the intercept compared to the scattering. This is the result of the extrapolation to zero chloride concentrations. Especially, the negative intercept found for 20 mol % $\mathbf{C_{10}C_{10}}^{-}$ is worrying because this results in a negative value for K_{OH}^{Cl}. Therefore, in Figure 6 the same data has been plotted, but instead of fitting to a linear equation the data has been fitted to the inverse of a linear equation ($y = 1/(a + bx)$). In this way, the scattering in the data points at high chloride concentrations are of less importance. The results are shown in Table 1. From the values of 100 mol % $\mathbf{C_{18}C_{18}}^{+}$ and 35 mol % $\mathbf{C_{10}C_{10}}^{-}$ of both the linear and nonlinear fits, the weight-averaged value for K_{OH}^{Cl} was calculated to be 2.4 ± 4.6. This value is somewhat smaller than that found in the literature (4−11).[36,39−43] However, for all but one study[43] these values have been measured for micellar

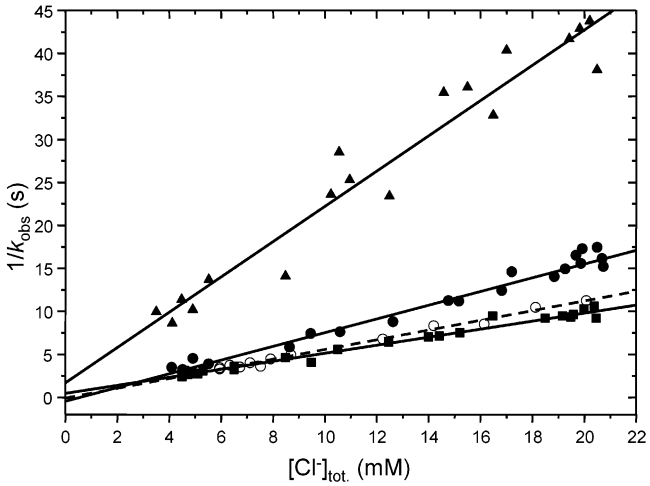

Figure 5. Linear plots used to calculate K_{OH}^{Cl} (eq 12). The percentage denotes the percentage of $\mathbf{C_{10}C_{10}}^{-}$ as a function of the total amphiphile concentration. (■) 0 mol %; (●) and (○) 20 mol %; (▲) 35 mol %.

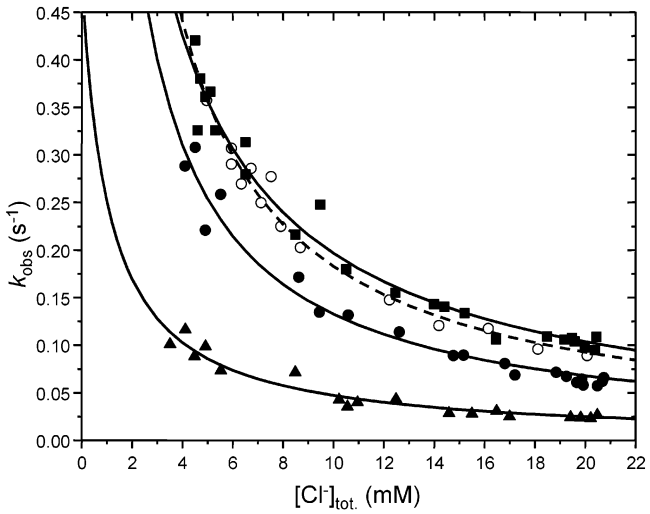

Figure 6. Nonlinear plots used to calculate K_{OH}^{Cl} (eq 12). The percentage denotes the percentage of $\mathbf{C_{10}C_{10}}^{-}$ as a function of the total amphiphile concentration. (■) 0 mol %; (●) and (○) 20 mol %; (▲) 35 mol %.

Table 1. Values of K_{OH}^{Cl} Obtained from Linear and Non-linear Fits

solution	linear fit	nonlinear fit
100% $\mathbf{C_{18}C_{18}}^{+}$	2.59 ± 0.26	1.96 ± 0.60
20% $\mathbf{C_{10}C_{10}}^{-}$	−14.17 ± 4.80	9.04 ± 16.06
20% $\mathbf{C_{10}C_{10}}^{-}$	−4.01 ± 3.52	3.52 ± 4.10
35% $\mathbf{C_{10}C_{10}}^{-}$	2.71 ± 4.43	2.11 ± 1.04

(36) García-Río, L.; Hervés, P.; Leis, J. R.; Mejuto, J. C.; Perez-Juste, J. *J. Phys. Org. Chem.* **1998**, *11*, 584−588.
(37) Keiper, J.; Romsted, L. S.; Yao, J.; Soldi, V. *Colloids Surf., A* **2001**, *176*, 53−67.
(38) Ruan, K.; Zhao, Z.; Ma, J. *Colloid Polym. Sci.* **2001**, *279*, 813−818.

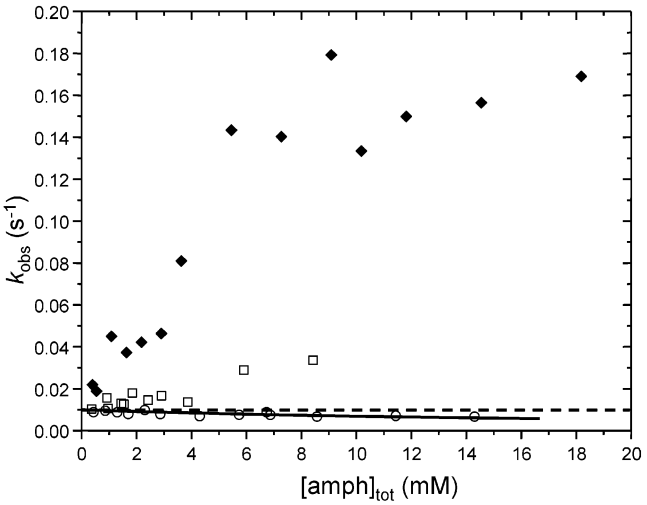

Figure 7. Experimental values for k_{obs} as a function of the total amphiphile concentration. The solid line is the least-squares fit of eq 13 to the data. The dashed line denotes the observed rate constant in pure water. The number denotes the percentage of $\mathbf{C_{10}C_{10}}^-$ as a function of the total amphiphile concentration. (◆) 45 mol %; (□) 50 mol %; (○) 70 mol %.

systems. It is not too surprising that the value of K_{OH}^{Cl} is independent of bilayer composition because this has also been observed for mixed micelles of cetyltrimethylammonium bromide (CTAB) and pentanol.[44]

Figures 1 and 7 show the plots of the observed rate constant versus the total amphiphile concentration. The scattering in the experimental data is large compared to the scattering observed for micellar solutions, but this is quite common for vesicular media.[36,45,46] As can be seen clearly, the maximum observed rate constant decreases with increasing $\mathbf{C_{10}C_{10}}^-$ content. Remarkably, the observed rate constant for the solution containing 50 mol % $\mathbf{C_{10}C_{10}}^-$ still shows an *increase* with increasing amphiphile concentration. This indicates that the outer leaflet must be slightly positive, since otherwise inhibition should occur. This inhibition is shown for 70 mol % $\mathbf{C_{10}C_{10}}^-$ (Figure 7) for which eq 6 simplifies to eq 13

$$k_{obs} = \frac{k_w[OH]_{tot}}{1 + K_S[amph]_{tot}} \qquad (13)$$

In principle, the increase in observed rate constant for 50% $\mathbf{C_{10}C_{10}}^-$ could be a salt effect because we use the sodium salt of $\mathbf{C_{10}C_{10}}^-$ and the chloride salt of $\mathbf{C_{18}C_{18}}^+$. However, the data in Figure 8 clearly shows that salt does not increase the observed rate constant for the Kemp elimination.

Considering that the increase in observed rate constant for 50 mol % $\mathbf{C_{10}C_{10}}^-$ is modest compared to that for 45 mol % $\mathbf{C_{10}C_{10}}^-$, it appears that the asymmetric amphiphile distribution is only in the range of 1 to 2 mol %.

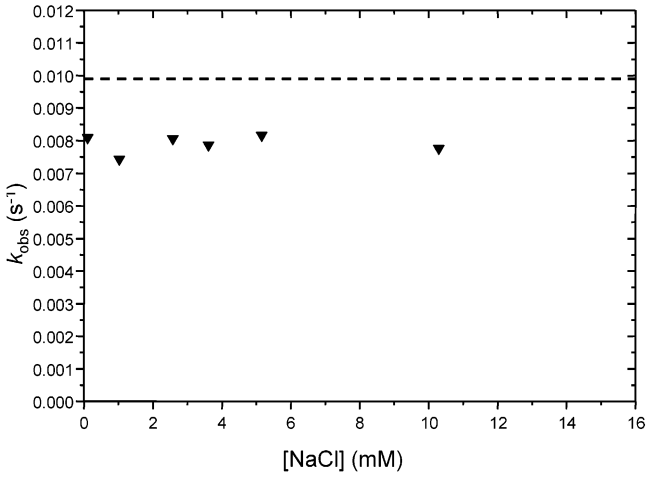

Figure 8. Experimental values for k_{obs} as a function of concentration NaCl. The dashed line is the observed rate constant in pure water.

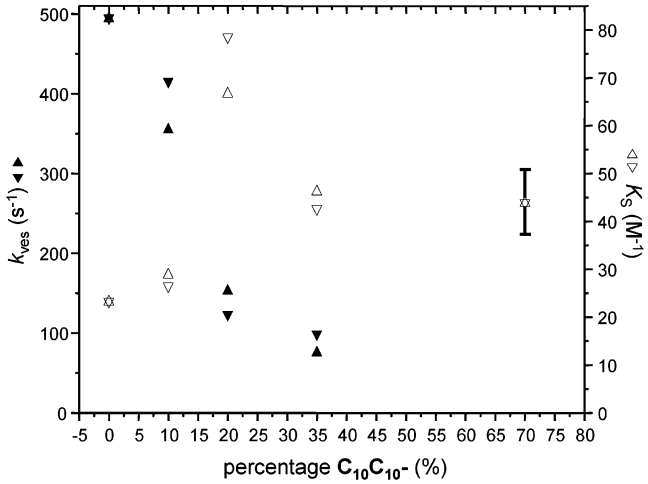

Figure 9. Plot of k_{ves} (left axis) and K_S (right axis) as a function of bilayer composition. Closed symbols are k_{ves} and open symbols K_S. Up triangles are from the fit with $\beta_{excess} = 0.8$ and down triangles are from the fit where β_{excess} increases from 0.8 for 0 mol % $\mathbf{C_{10}C_{10}}^-$ to 1 for 50 mol % $\mathbf{C_{10}C_{10}}^-$. Error bars represent the error in the fit to eqs 6 and 8.

The data for 45 mol % $\mathbf{C_{10}C_{10}}^-$ and 50 mol % $\mathbf{C_{10}C_{10}}^-$ were not fitted to eq 6, because the experimental profiles only show the beginning of the rate profile, resulting in an unreliable fit. Performing the kinetic experiments at higher amphiphile concentration was not possible because of solubility problems.

We fitted the data of 100 mol % $\mathbf{C_{18}C_{18}}^+$, 10 mol % $\mathbf{C_{10}C_{10}}^-$, 20 mol % $\mathbf{C_{10}C_{10}}^-$, 35 mol % $\mathbf{C_{10}C_{10}}^-$ and 70 mol % $\mathbf{C_{10}C_{10}}^-$ using $K_{OH}^{Cl} = 2.4$. The fits are shown in Figures 1 and 7. A plot of the binding constant and vesicular rate constant as a function of the $\mathbf{C_{10}C_{10}}^-$ content is given in Figure 9. The data have been fitted keeping β_{excess} constant at 0.8,[11] or fitted with β_{excess} increasing slowly from 0.8 to 1. The reason for the latter fit is that upon increasing the $\mathbf{C_{10}C_{10}}^-$ content the ratio of chloride concentration to the concentration of excess $\mathbf{C_{18}C_{18}}^+$ is also increasing, resulting in a higher counterion binding. However, the influence of this increasing counterion binding on the fits is only modest compared to the fits with constant counterion binding and has no influence on the general trend.

At this stage we note that the formation of microdomains at 10−30 mol % of $\mathbf{C_{10}C_{10}}^-$ (as indicated by DSC, Figure 3) will influence the composition-dependent rate constants shown in Figure 9. However, we refrain from a further analysis of this

(39) Chaimovich, H.; Bonilha, J. B. S.; Politi, M. J.; Quina, F. H. *J. Phys. Chem.* **1979**, *83*, 1851−1854.
(40) Romsted, L. S. In *Surfactants in Solution*; Mittal, K. L., Lindman, B., Eds.; Plenum Press: New York, 1984; pp 1017−1065.
(41) Bartet, D.; Gamboa, C.; Sepúlveda, L. *J. Phys. Chem.* **1980**, *84*, 272−275.
(42) Al-Lohedan, H.; Bunton, C. A.; Romsted, L. S. *J. Phys. Chem.* **1981**, *85*, 2123−2129.
(43) Kawamuro, M. K.; Chaimovich, H.; Abuin, E. B.; Lissi, E. A.; Cuccovia, I. M. *J. Phys. Chem.* **1991**, *95*, 1458−1463.
(44) Rodríguez, A.; Múñoz, M.; Graciani, M. D. M.; Moyá, M. L. *J. Colloid Interface Sci.* **2002**, *248*, 455−461.
(45) Brinchi, L.; di Profio, P.; Germani, R.; Marte, L.; Savelli, G.; Bunton, C. A. *J. Colloid Interface Sci.* **2001**, *243*, 469−475.
(46) Khan, M. N.; Ismail, E.; Misran, O. *J. Mol. Liq.* **2002**, *95*, 75−86.

effect in the absence of more detailed information about the size of these domains.

Because the deprotonation reaction is general-base catalyzed, the phosphate headgroup might catalyze the reaction as well. However, this was ruled out for two reasons: (1) we do not observe any catalysis by anionic vesicles; (2) the relative pK_a of water and dialkyl phosphate is 15 and 5 (rough estimate),[47] respectively. Given that the Brønsted β value for the kinetic probe in this study is 0.74[23] this leads a factor of at least $10^{7.4}$ in rate difference between the phosphate-catalyzed reaction and the hydroxide-catalyzed reaction. Thus, the phosphate catalyzed reaction can be neglected compared to the hydroxide catalyzed reaction.

To further support our kinetic analysis we have made an independent study of the polarity of the vesicular binding sites, the counterion binding to the bilayers and the ζ-potentials of the bilayers.

Bilayer and Binding Site Polarity. The binding constant of the kinetic probe between 0 mol % $\mathbf{C_{10}C_{10}}^-$ and 70 mol % $\mathbf{C_{10}C_{10}}^-$ stays about the same (considering the scattering in the data), whereas the vesicular rate constant decreases strongly. This is remarkable because the vesicular rate constant depends mainly on the polarity of the vesicular reaction medium. We expected that the polarity of the bilayer would change only modestly with increasing $\mathbf{C_{10}C_{10}}^-$ content.

Therefore we decided to use both pyrene and Reichardt's E_T-(30)-probe to study the bilayer polarity. The ratio of the intensities of the first and third vibronic peak in the emission spectrum of pyrene (I_1/I_3) gives an indication of the local polarity that the probe senses.[48] Hydrocarbon solvents generally have an I_1/I_3-value around 0.6, aromatic solvents between 1.00 and 1.30 and simple polar solvents between 1.30 and 2.00.[48] Recently, evidence has been found that polyaromatic probes might be in a fast equilibrium between the headgroup area and the inner core of cationic and nonionic micelles.[49−51]

The E_T(30)-probe has been used to measure the polarity of a wide variety of solvents, solvent mixtures and aggregates.[28] The interactions with the environment are slightly more complex because it is not only sensitive to medium polarity, but also to hydrogen bond donation. Compared to pyrene, the probe molecule is also larger, and therefore more bilayer disturbing. However, still valuable information on supramolecular aggregates can be obtained. Figure 10 shows the dependence of both the E_T(30)-value and I_1/I_3 as a function of bilayer composition. For the E_T(30) probe the increase in polarity can be explained by the displacement of the probe out of the bilayer with increasing $\mathbf{C_{10}C_{10}}^-$ content. The positive charge in the probe is relatively (sterically) hidden from its environment, while the negative charge is readily accessible. This results in a favorable interaction with positively charged vesicles, but with an unfavorable interaction with negatively charged vesicles. Therefore, at high $\mathbf{C_{10}C_{10}}^-$ content (>30 mol %) the probe will be (partly) expelled into the bulk water. The increase in E_T(30) value of approximately 3 kcal/mol going from cationic to anionic vesicles is similar to the increase observed going from cationic to anionic micelles.[52] Unfortunately, no quantitative explanation for this latter observation has been given.

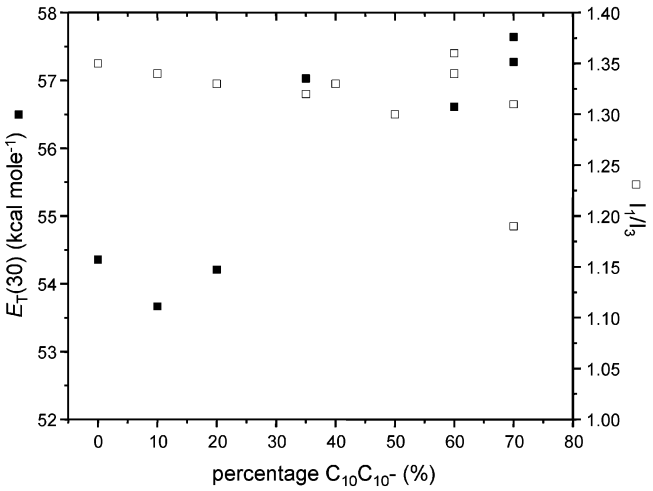

Figure 10. Plot of E_T(30) (■; left axis) and I_1/I_3 (□; right axis) as function of bilayer composition.

Upon increasing the $\mathbf{C_{10}C_{10}}^-$ content in the vesicles, the I_1/I_3 value stays more or less constant. This suggests that that the local polarity of the bilayer sensed by pyrene is about constant throughout the whole amphiphile composition range used in the kinetic studies.

Of course, the binding location of our kinetic probe is important as well because the pseudophase model does not take different binding sites into account. However, we contend that due to the polar groups in the kinetic probe, it binds close to the aqueous interface and does not change location upon going to more negatively charged bilayer compositions.

Counterion Binding. Kinetic studies show that in cationic micelles the micellar rate constant does not vary much upon the addition of butanol,[53,54] pentanol[44] or $C_{10}E_4$.[6] Instead, the decrease in *observed* rate constant is attributed to a decrease in counterion binding. This decrease in counterion binding is confirmed for mixed micelles of anionic surfactants and alcohols[9] and nonionic surfactants.[55] However, care has to be taken because certain nonionic amphiphiles increase the micellar rate constant.[56]

On the basis of these results, we decided to fit the data again, but keeping constant the vesicular rate constant and the binding constant (using the data from the fit of 100 mol % $\mathbf{C_{18}C_{18}}^+$), thus allowing β_{excess} to vary. Apart from the literature evidence, this can be rationalized by the fact that the counterion binding for aggregates with only one type of amphiphile (positive or negative), is high, because there is a high local charge density. When cationic and anionic amphiphiles are mixed in unequal amounts, the overall local charge density is lowered and then a high counterion binding is not needed.

(47) Serjeant, E. P.; Dempsey, B. *Ionisation Constants of Organic Acids in Aqueous Solution*; Pergamon Press: Oxford, 1979.
(48) Kalyanasundaram, K.; Thomas, J. K. *J. Am. Chem. Soc.* **1977**, *99*, 2039−2044.
(49) Cang, H.; Brace, D. D.; Fayer, M. D. *J. Phys. Chem. B* **2001**, *105*, 10 007−10 015.
(50) Matzinger, S.; Hussey, D. M.; Fayer, M. D. *J. Phys. Chem. B* **1998**, *102*, 7216−7224.
(51) Honda, C.; Itagaki, M.; Takeda, R.; Endo, K. *Langmuir* **2002**, *18*, 1999−2003.
(52) Zachariasse, K. A.; Van Phuc, N.; Kozankiewicz, B. *J. Phys. Chem.* **1981**, *85*, 2676−2683.
(53) Bertoncini, C. R. A.; Nome, F.; Cerichelli, G.; Bunton, C. A. *J. Phys. Chem.* **1990**, *94*, 5875−5878.
(54) Bertoncini, C. R. A.; Neves, M. D. S.; Nome, F.; Bunton, C. A. *Langmuir* **1993**, *9*, 1274−1279.
(55) Rathman, J. F.; Scamehorn, J. F. *J. Phys. Chem.* **1984**, *88*, 5807−5816.
(56) Blaskó, A.; Bunton, C. A.; Toledo, E. A.; Holland, P. M.; Nome, F. *J. Chem. Soc., Perkin Trans. 2* **1995**, 2367−2373.

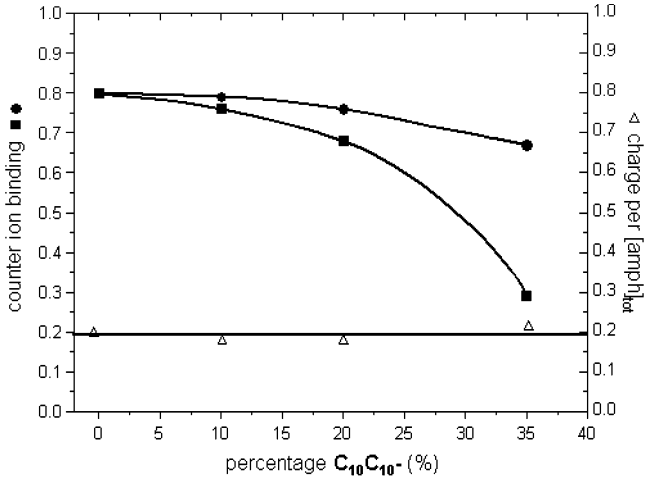

Figure 11. Plot of the *total* counterion binding (●; left axis), the *excess* counterion binding (■; left axis) and charge per *total* amphiphile concentration (△; right axis) as a function of bilayer composition. Lines are drawn to guide the eye.

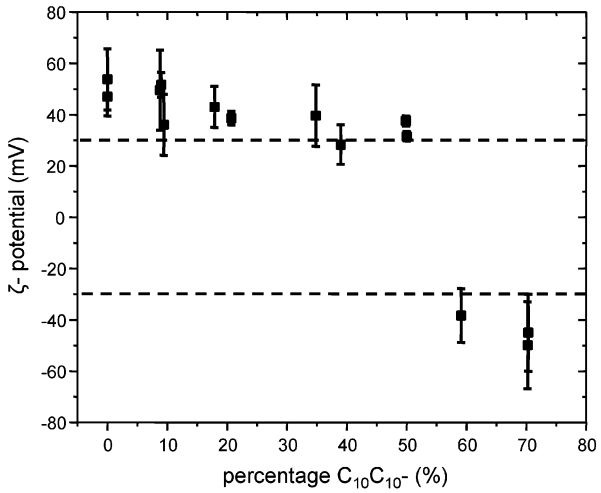

Figure 12. Plot of the ζ-potential as function of the bilayer composition. The error bars denote the width of the ζ-potential peak.

Figure 11 shows the *excess* counterion binding as a function of the $\mathbf{C_{10}C_{10}}^-$ content. The calculated *total* counterion binding (β_{tot}; eq 11) is shown as well. Surprisingly, this total counterion binding is only slightly affected by the addition of $\mathbf{C_{10}C_{10}}^-$. By contrast, the *excess* counterion binding is significantly decreased upon addition of $\mathbf{C_{10}C_{10}}^-$, and we contend that the kinetic data shown in Figures 1 and 7 are primarily determined by this factor. The excess counterion binding for 35 mol % of $\mathbf{C_{10}C_{10}}^-$ is quite low (0.29), but reasonable compared to that for mixed micelles of CTAB and nonionic amphiphiles[6,56] or butanol.[53]

Surface and ζ-Potential. The surface charge density (charge per area; σ_0) is given by eq 14 because both $\mathbf{C_{10}C_{10}}^-$ and $\mathbf{C_{18}C_{18}}^+$ have comparable headgroup areas

$$\sigma_0 = \frac{n_{\text{charge}} e}{n_{\text{amph}} a_0} \tag{14}$$

In this equation n_{charge} and n_{amph} are the number of charges and the number of amphiphiles, respectively. a_0 is the cross-sectional headgroup area and e the charge unit. The surface charge is related to the charge per total amphiphile concentration (e_{amph}; eq 15) because the surface charge arises from cationic amphiphiles that do not have a counterion or adjacent anionic amphiphile in their vicinity to compensate their charge

$$e_{\text{amph}} = \frac{(1-\beta_{\text{excess}})(1-2\alpha)[\text{amph}]_{\text{tot}}}{[\text{amph}]_{\text{tot}}} \tag{15}$$

Calculation of the charge per total amphiphile concentration (Figure 11) shows that the charge per amphiphile stays about constant between 0 mol % and 35 mol % of $\mathbf{C_{10}C_{10}}^-$. This suggests that changes in the vesicular rate constant will be small.

The ζ-potential is the potential measured at the slipping plane of a particle moving through a solution and is related to the surface charge.[57] However, this parameter is not entirely free of ambiguity. The main problem is that the distance from the surface to the slipping plane depends on several parameters, e.g., pH, salt concentration and particle size.[58] In our series of bilayer compositions, the pH is kept constant, but the salt concentration is increased going to higher percentages of $\mathbf{C_{10}C_{10}}^-$ because we add the sodium salt of $\mathbf{C_{10}C_{10}}^-$ to the chloride salt of $\mathbf{C_{18}C_{18}}^+$. However, despite these difficulties and complexities we assume that there is a relationship between the ζ-potential and the charge per amphiphile (and β_{tot}). As can be seen in Figure 12 the ζ-potential only slightly decreases with increasing $\mathbf{C_{10}C_{10}}^-$ content, which is consistent with the about constant value of charge per amphiphile and the slightly decreasing value of β_{tot}.

One might anticipate that the ζ-potential should decrease more strongly since the surface potential is decreased upon the addition of more $\mathbf{C_{10}C_{10}}^-$, but at the same time also the salt concentration is increased, and therefore, the ζ-potential is measured closer to the vesicular surface. Apparently, these two effects compensate each other, and the ζ-potential is only slightly decreased.

Special attention should be drawn to the ζ-potential for 50 mol % $\mathbf{C_{10}C_{10}}^-$. For this solution the ζ-potential is approximately 30 mV indicating that the outer leaflet is positively charged and the aggregates are colloidally stable. This is in agreement with the catalytic effect found for this solution. In our system, catalysis should be shown only for positively charged aggregates and inhibition is anticipated for nonionic and anionic aggregates. Therefore, these ζ-potential measurements are fully consistent with our kinetic results.

We recall that the *vesicular* rate constant depends on the composition of the bilayer as well, but only to a small extent. Unfortunately, the model and the scattering in the data do not allow us to vary all three parameters independently: k_{ves}, K_S, and β_{excess}. Therefore, we anticipate that the most realistic fits are between the two extreme cases we examined here, i.e., the case where we vary either K_S and k_{ves} or where we vary β_{excess}. However, on the basis of the polarity and ζ-potential experiments, we expect the combination of a constant vesicular rate constant (k_{ves}) and binding constant of the kinetic probe (K_S) is closest to the most realistic fit, and it is primarily the decrease of β_{excess} that determines the catalytic effect.

(57) Hiemenz, P. C. In *Principles of Colloid and Surface Chemistry*; Marcel Dekker: New York, 1977; pp 453−487.

(58) Carmona-Ribeiro, A. M.; Midmore, B. R. *J. Phys. Chem.* **1992**, *96*, 3542−3547.

Conclusions

Vesicles prepared from $\mathbf{C_{18}C_{18}}^+$ efficiently catalyze the Kemp elimination. The experimental data can be analyzed using the pseudophase model with ion exchange. From the fit for 100 mol % $\mathbf{C_{18}C_{18}}^+$, it is calculated that the vesicular rate constant is approximately 65 times larger than the water rate constant. Upon the introduction of increasing amounts of $\mathbf{C_{10}C_{10}}^-$ into the bilayer, the observed catalysis (maximum observed rate constant) is decreased. Experiments with Reichardt's $E_T(30)$ probe and pyrene indicate that the polarity of the bilayer surface area is independent of the composition for these binary amphiphile mixtures. Therefore, the vesicular rate constant and the binding constant of the kinetic probe to the bilayer should be constant as well. The kinetic data are fitted using these observations. From these fits, it is concluded that the counterion binding to the excess cationic amphiphiles is decreased as a result of a decrease in the local charge density. The catalytic efficiency upon adding $\mathbf{C_{10}C_{10}}^-$ to the cationic vesicle primarily responds to this decrease of the excess counterion binding. At 50 mol % $\mathbf{C_{10}C_{10}}^-$, the outer leaflet of the vesicles is slightly positively charged as is indicated by the fact that these vesicles still show catalysis. Inhibition is observed for negatively charged vesicles, as for example for vesicles containing 70 mol % of $\mathbf{C_{10}C_{10}}^-$.

Finally, differential scanning microcalorimetry shows that between 5 mol % and 30 mol % $\mathbf{C_{10}C_{10}}^-$, neutral microdomains exist in the bilayer. It is concluded that, like in biological membranes, also in bilayers made from synthetic amphiphiles "raft" (microdomain) formation can occur.

In the present study, we have made an attempt to identify the kinetic complexities which arise in the kinetic data when vesicles formed from a single bilayer-forming amphiphile are replaced by vesicles containing variable amounts of another bilayer forming amphiphile of opposite charge-type. This approach represents a first step toward examining bilayer compositions that are more akin to those found in biological membranes.

Acknowledgment. We thank Prof. L. S. Romsted (State University of New Jersey, New Jersey, USA) and Prof. M. J. Blandamer (University of Leicester, Leicester, UK) for fruitful discussions. We thank Dr. M. C. A. Stuart (University of Groningen) for taking the cryo electron microscopy pictures. The National Research School Combination Catalysis is acknowledged for the financial support.

JA027772A